Supplementary materials

MARCH4 in pollutant-repressed MHC-I and plasticity of lung squamous cancer

Gui-Zhen Wang[1,2*], Xiao-Liang Jie[1*], Guo-Chao Zhang[3*], Zi-Han Sun[4], Aikede Alifu[1], Zheng Wang[1], Zhen-Yi Wang[5], Yu-Ke Shen[1], Yi-Meng Zhang[1,6], Fen-Rong Xie[1,6], Meng-Yao Lv[1], Liu Ye[1,6], Cong Wang[1], Bing-Qing Xu[1], Yong-Fang Lin[1], Yan-Yun Gao[2], Yang-Tong Liu[1], Yi-Shuai Tan[1],Yan-Zhi Bai[1], Yu-Da Zhao[7], Jian-Hua Chang[8], You-Sheng Mao[3], Qi Xue[3], Yun-Chao Huang[9], Jian-Ming Ying[4], Yu-Tao Liu[1] (✉), Feng-Wei Tan[3] (✉), Guang-Biao Zhou[1,2] (✉)

This file contains 9 supplementary tables and 11 supplementary figures.

Materials and methods

Patients and samples

The study was approved by the research ethics committee of the Cancer Hospital, Chinese Academy of Medical Sciences (NCC2020A190) and was conducted in accordance with the tenets of the Declaration of Helsinki. All samples were collected with informed consent. The diagnosis of NSCLC was confirmed by at least two pathologists. Formalin-fixed, paraffin-embedded tissue sections (5 μm) were obtained from the Department of Pathology of our hospital, and tissue microarrays were supplied by Xinchao Biotech (Shanghai, China). Tissue samples were collected from 233 patients with benign lung diseases or LUSC, and details of patient demographics and clinical information are provided in Tables S1-S6.

To determine the efficacy of ATRA in adult patients, it was used as a neoadjuvant therapy in combination with ICIs and platinum-based doublet chemotherapy for resectable stage IIA to IIIB LUSCs. The study was approved by the Ethics Committee of our hospital (approval No. 24/549-4829) and informed consent was obtained from every patient. ATRA (20 mg orally, three times daily) was initiated one week before the first dose of ICIs and continued thereafter. ICIs and chemotherapy were administered intravenously in 3-week cycles. The platinum agent was either carboplatin (AUC 4-5, n=7) or, in cases of intolerance, cisplatin (75 mg/m², n=1). Investigators selected one of the following agents per patient characteristics: liposomal paclitaxel (175 mg/m², n=3) or albumin-bound paclitaxel (260 mg/m², n=5). Among the eight patients, one case received two cycles and seven cases received three cycles of this regimen. Tumor samples were harvested via transbronchoscopic lung biopsies (before treatment) or surgical resection (after treatment) for H&E and periodic acid-Schiff (PAS) staining, and

mIHC assays.

Cell culture and reagents

The human lung cancer cell lines H520, H1703, A549, H226, and SKMES-I, murine lung cancer cell lines M109, KLN205, the human normal bronchial epithelial Beas-2B cell line, embryonic lung fibroblasts (HLF), and human embryonic kidney HEK-293 cells were obtained from the American Tissue Culture Collection (ATCC, Manassas, VA, USA). The human normal bronchial epithelial 16HBE cell line was obtained from the Clonetics (Walkersville, MD, USA). The cells were cultured in DMEM or RPMI-1640 supplemented with 10% fetal bovine serum (Gibco/BRL, Grand Island, NY, USA). Cells were treated with CSE that was prepared by a modified method of Carp and Janoff (*1, 2*), $PM_{2.5}$ that were dissolved in DMSO, representative carcinogens (Table S7), or clinically available drugs (Table S8) with indicated protocols. After treatment, the cells were harvested, and analyzed. The cells were also transfected with 50 nmol/L double-stranded siRNAs/shRNAs (Table S9) or indicated plasmids using HiPerFect Transfection Reagent (Qiagen, Crawley, UK). To evaluate changes in cell morphology, coverslips were placed in culture plates to allow the cells to grow on them.

Cell morphology and PAS Staining

The adherent cells grew on coverslips were fixed with 4% paraformaldehyde for 30 min and permeabilized with 0.5% Triton X-100 for 20 min. Subsequently, cells were subjected to H&E staining and examined under a microscope. The nuclear area of the cells was quantified using the HALO® software (version 4.1; Indica Labs, Albuquerque, NM, USA). PAS staining was performed to detect polysaccharides in goblet or goblet-like cells. For periodic

acid–Schiff (PAS) staining (Abcam, ab150680), 5 μm paraffin sections were deparaffinised in xylene and rehydrated to water. Following 5 min oxidation in 1 % periodic acid and four distilled-water rinses, sections were incubated in Schiff reagent for 15 min, developed in hot (37 °C) tap water, counterstained with modified Mayer's hematoxylin for 2–3 min, blued in 0.1 % ammonium water, counterstained with 0.1 % light green for 2 min, dehydrated, cleared and mounted in synthetic resin. Images were acquired and approximately 2,500 cells were analyzed using HALO software (Indica Labs) to quantify PAS-positive cells.

Plasmid Construction and Transfection

MARCH4 cDNA was PCR-amplified using 2×Phanta Max Master Mix (Vazyme, Nanjing, China) and cloned into pCDH-CMV-GFP, pcs2-HA, Flag-tag, or pcDNA3.1 vectors. For lentiviral-mediated knockdown, shRNA sequences (Table S8) targeting *MARCH4* were inserted into the pLKO.1-puro vector (Addgene, Watertown, MA, USA). Non-targeting scramble shRNAs were used as negative controls. Recombinant lentiviruses were generated by co-transfection of shRNA plasmids and packaging plasmids pMD2.G and psPAX2 into HEK293T cells. Viral supernatants were harvested 48-72 h post-transfection, filtered (0.45 μm), and used for infection. H520 cells were transfected with lentivirus in the presence of polybrene and selected with 2 μg/ml puromycin for 7 days to establish specific gene stable knockdown cell lines.

Luciferase reporter assay

The promoter region of *MARCH4*, -1000 upstream of the initiating ATG codon, was amplified by PCR and cloned into pGL3-promoter plasmid. HLF cells were transfected with plasmids containing *MARCH4* promoter-driven luciferase, with or without BaP treatment.

After 48 h, luciferase activity was measured using a Dual-Luciferase Reporter Assay System (Promega, Madison, WI, USA).

Immunohistochemistry (IHC) and multiplex IHC (mIHC) assays

Formalin-fixed, paraffin-embedded (FFPE) human or mouse lung specimens (5 μm) were deparaffinized and subjected to a heat-induced epitope retrieval using a microwave. The sections were blocked with 5% bovine serum albumin (BSA), followed by an overnight incubation at 4°C with the primary antibody. After washing, sections were incubated with the secondary antibody. The slides were dehydrated, cleared, and counterstained with hematoxylin. Detection was performed using 3,3'-diaminobenzidine (Zhongshan Golden Bridge, Beijing, China). The immunoreactivity score (IRS) was calculated as IRS (0-12) = RP (0 – 4) × SI (0 – 3), where RP is the ratio of positive-staining cells and SI is the staining intensity. For mIHC, sections were incubated with appropriate primary antibodies overnight at 4°C. After washing, corresponding fluorophore-conjugated secondary antibodies were applied for 10 – 15 minutes. Additional staining rounds were performed as needed to detect all target proteins. Nuclei were counterstained with DAPI. Sections were mounted with an anti-fade medium and imaged using a Leica fluorescence microscope. Multi-color fluorescent images were captured and analysed with HALO software to quantify the colocalization and expression patterns of target proteins, and X-tile software was used to determine the optimal cutoff value for dichotomizing patients into high and low MHC-I expression groups.

GST-Pull down

Recombinant GST-fused HLA-A (residues 22-365 aa), HLA-B (1-362 aa), and HLA-C (1-336 aa) proteins were synthesized with a wheat germ cell-free expression system (Abnova,

Taibei, China) and affinity-purified with Glutathione Sepharose 4B resin (GE Healthcare, Fairfield, CO, USA; Cat#17075601) according to the manufacturer's protocol. Protein concentrations were determined by BCA assay (Thermo Fisher Scientific, Basingstoke, UK, Cat# 23225). For pull-down experiments, 20 μg of GST or GST-HLA proteins were pre-incubated with 30 μL of Glutathione Sepharose 4B beads (pre-equilibrated in binding buffer) for 4-6 h at 4 °C with gentle rotation. After washing three times with binding buffer, the beads were incubated with purified Flag-MARCH4 protein overnight at 4 °C. Unbound proteins were removed by six washes with 1 mL of ice-cold washing buffer. Finally, the agarose beads were boiled with 1× SDS loading buffer for 10 min and analyzed by western blotting. Antibodies used in this study are listed in Table S10.

Proximity ligation assay (PLA)

PLA was performed according to the Duolink in situ Fluorescence protocol (Sigma–Aldrich, St. Louis, MO, USA). Briefly, cells were fixed with 4% paraformaldehyde in PBS, washed, permeabilized, and washes. Cells were blocked with a blocking solution and incubated with specific primary antibodies overnight. After washes, cells were incubated with diluted PLA probes and washed. Ligation was performed by incubating the cells with the ligation solution, washed, and incubated with the amplification solution. The reaction was stopped by two washes with Wash Buffer, mounted onto slides using a mounting medium containing DAPI and dried. Slides were imaged using a fluorescence microscope with DAPI and Texas Red filters. Images were visualized with a Nikon N-STORM Super-Resolution confocal laser scanning microscope.

Isolation of DCs and $CD8^+$ T cells and co-culture with tumor cells

Peripheral blood mononuclear cells (PBMCs) were isolated from 10 mL of anticoagulated whole blood collected from healthy donors using Ficoll density gradient centrifugation. $CD8^+$ T cells and monocytes were subsequently separated from the PBMCs by magnetic bead-based separation. The $CD8^+$ T cells were cultured in X-vivo complete medium (Gibco) supplemented with serum and IL-2. The monocytes were induced to differentiate into DCs by culture in RPMI-1640 complete medium containing recombinant human granulocyte-macrophage colony-stimulating factor (GM-CSF, 1000 U/mL) and IL-4 (1000 U/mL). Immature DCs were harvested on day 6 of culture. To allow for antigen uptake and T cell activation, 5×10^4 DCs and 5×10^5 $CD8^+$ T cells were added to 24-well plates containing pre-adhered 1×10^5 H520 cells. After 48 h, flow cytometry was performed to analyse the $GZMB^+$ and $perforin^+$ cells within the $CD8^+$ T cell population.

Flow Cytometry

Tumor tissue samples from mice were sectioned into 2-3 mm fragments and digested with 0.3% collagenase IV (Sigma–Aldrich) to obtain single-cell suspensions. The cells were filtered through a 100-micron stainless steel mesh to remove clumps. The cells were blocked with CD16/32 monoclonal antibody (TruStain fcX, BioLegend), incubated with the specified antibodies (Table S10), washed, and analyzed with a Cytek NL-CLC3000 flow cytometer (Cytek, Shanghai, China). Matched isotype controls were included in all experiments, and representative gating strategy is shown in Fig. S10m.

Co-immunoprecipitation and Western blot assays

Cell lysates were extracted in IP lysis buffer at 4 °C for 30 min, supernatants were clarified by centrifugation at 12,000 g for 15 min. The specified antibody was added to the lysates and

incubated overnight at 4 °C. Protein A/G PLUS-Agarose (Santa Cruz Biotechnology, Santa Cruz, CA, USA) were added, followed by a 6-h incubation. The beads were washed 5-6 times with IP lysis buffer, boiled with 2× SDS-PAGE loading buffer for 10 minutes. The input lysates and immunoprecipitates were separated by 5%-15% SDS-PAGE and analyzed by Western blotting using indicated antibodies (Table S10).

Transmission electron microscopy (TEM)

Freshly isolated cell pellets (1×10^7 cells) were immediately fixed in 2.5% glutaraldehyde in 0.1 M PBS at 4 °C for 12 h. After three 15-min rinses with the same buffer, specimens were post-fixed with 1% osmium tetroxide in PBS for 2 h at room temperature, followed by three additional washes with 0.1 M PBS. Dehydration was performed through a graded ethanol series (30%, 50%, 70%, 90%, 100%; 15 min each) and completed in propylene oxide (10 min, twice). Samples were embedded and polymerized at 70 °C for 48 h. Ultrathin sections (70–90 nm) were cut with a diamond knife on an ultramicrotome (Leica UC7) and collected on 200-mesh copper grids. Sections were contrast-stained with 2% uranyl acetate (8 min) and Reynolds' lead citrate (5 min), dried under a dust-free environment, and examined with a HITACHI TEM operated at 80 kV. Images were acquired using a CCD camera.

Screening for agents that upregulate MHC-I

The FDA-approved Anticancer Drug Library (L2000, Selleck Chemicals LLC, Houston, TX, USA; Table S8) was screened for drugs that are able to upregulate MHC-I. 16HBE cells (5×10^4 cells/well) were seeded in 24-well plates and cultured overnight. Cells were treated with compounds at 5 μM or vehicle control for 48 h. MHC-I surface expression was analyzed by flow cytometry using an APC-conjugated anti-MHC-I antibody (clone W6/32, BioLegend).

Relative mean fluorescence intensity (MFI) was normalized to vehicle-treated controls. Microvilli and secretary vesicles were counted.

Patient-derived organoids

Freshly isolated human LUSC tumors were minced into 5-mm^3 fragments and enzymatically digested for 1 h at 37°C in DMEM/F12 (Gibco) containing 1.0 mg/ml collagenase I (Gibco) and 0.5 mg/ml collagenase IV (Gibco) with mechanical trituration every 15 min. After filtration through 70-μm strainers and ACK lysis, cells were pelleted, resuspended in ice-cold Matrigel (Corning, NY, USA), and plated as 40-μl drops (5×10^4 cells) in 48-well plates. Following 15 min solidification, pre-warmed organoid culture medium was added. Established organoids were maintained in 6-well plates (2 ml medium/well). For passaging, 20 μl of 100× Dispase solution was added per well and incubated at 37°C for 30 min. Organoids were collected, resuspended in fresh medium, mixed with Matrigel to 80% on ice, and replated as 200-μl droplets onto inverted pre-warmed 6-well plates. After 5–10 min at room temperature and 30–60 min incubation (inverted) at 37°C for polymerization, 2 ml fresh medium was added per well. For drug treatment experiments, ATRA and Bexarotene were added to the organoid culture medium at final concentrations of 10 μM, respectively. Control groups were treated with an equal volume of DMSO. After 15 days of treatment, organoids were harvested for H&E staining, mIHC, and qRT-PCR assays of indicated proteins/genes.

Animal studies

The animal studies were approved by the Ethics Committee of Cancer Hospital, Chinese Academy of Medical Sciences (ID: NCC2019A188). All animal studies were conducted according to protocols approved by the Ethics Committee. Female C57BL/6, BALB/c mice

and NCG mice (4-6 weeks old) were purchased from the GemPharmatech Co., Ltd (Nanjing, China). Homozygous AhR-deficient mice were purchased from the Jackson Laboratory (Bar Harbor, Maine, USA). The conditional *Ahr* allele (Ahr^{fx}) contains exon 2 of *Ahr* flanked by *loxP* sites ("floxed"), and the mice homozygous for the Ahr^{fxneo} allele were crossed with mice expressing Cre recombinase driven by the surfactant protein C promoter (SPC-Cre), resulting in *Ahr* deficiency in alveolar type II cells in the lungs. $March4^{-/-}$ mice were established by microinjection of sgRNAs targeting exon 2-4 of *Marchf4* gene as well as Cas9 mRNA into zygotes of C57BL/6J mice. Ferrets were maintained in a clean farm facility of Wuxi Sangoho Biotechnology Co., Ltd (Wuxi, Jiangsu, China).

The mice and ferrets were whole-body exposed to cigarette smoke. This regimen consisted of 12 cigarettes per day, 5 days per week for six months, with each cigarette exposure lasting 3 minutes and followed by a 15-minute period of fresh air. For establishment of LUSC mouse model, 5×10^6 KLN205 cells were subcutaneously inoculated into the dorsal flank of the mice using a trocar. Tumor size was measured every alternate day with electronic caliper, and when the tumors reached 50 mm^3, the mice were treated with ATRA/BXRT at 50 mg/kg/day, 5 days per week for 3 weeks, and/or αPD-L1 four times on days 7, 10, 13 and 16. The NCG mice were injected with 2×10^5 H520 cells via tail vein, and treated with ATRA at 50 or 100 mg/kg/day for 14 days. When tumors reached 2 cm, appeared moribund, or reached projected timepoints, animals were anesthetized with the mixture of oxygen/isoflurane inhalation and sacrificed by cervical dislocation. Lung tissues were excised, photographed, and subjected to H&E and IHC/mIHC staining.

Statistical analysis

All in vitro experiments were performed at least three times, and the results are presented as the means ± SD. All the statistical analyses were conducted using GraphPad Prism 9 (GraphPad Software, La Jolla, CA, USA). The survival curve for each group was estimated by the Kaplan-Meier method and log-rank test. Statistically significant differences were determined by Student's *t*-test, two-way ANOVA, or as indicated. *P* values less than 0.05 were considered statistically significant.

Data availability

The Cancer Genome Atlas (TCGA) RNA-seq data were downloaded from cBioPortal database (https://www.cbioportal.org/, with approval by the National Institutes of Health number #24437-4). The UK Biobank data were used (under Application Number 176137) to analyze the correlation between MHC-I expression levels and $PM_{2.5}$ concentrations. The $PM_{2.5}$ concentration data (field 24006) for 2010 in the UK Biobank were estimated via a Land Use Regression (LUR) model. This model was developed based on $PM_{2.5}$ monitoring data collected from January 26, 2010, to January 18, 2011, thus ensuring that the generated estimates were representative of the $PM_{2.5}$ exposure levels in 2010. Participants were filtered to retain a total of 8352 individuals who were enrolled between January 1 and December 31, 2010. A linear regression model was then applied to assess the correlation between $PM_{2.5}$ exposure and the summed Normalized Protein eXpression (NPX) values of HLA_A, HLA_E, and HLA_DRA. The regression model was fitted using the lm() function in R software. For each regression coefficient, R computes a t-statistic by dividing the estimated coefficient by its standard error, with the corresponding P-value derived from the t-distribution with the appropriate degrees of freedom. We further calculated the mean values for the 8347

232 participants with available assessment centre information, by aggregating data for individuals
233 belonging to the same assessment centre. Subsequently, the identical linear regression
234 approach was used to examine the relationship between population-averaged $PM_{2.5}$ and
235 population-averaged MHC molecule NPX values.
236

References

1. H. Carp, A. Janoff, Possible mechanisms of emphysema in smokers. In vitro suppression of serum elastase-inhibitory capacity by fresh cigarette smoke and its prevention by antioxidants. *Am Rev Respir Dis* **118**, 617–621 (1978).
2. G.-Z. Wang *et al.*, The Aryl hydrocarbon receptor mediates tobacco-induced PD-L1 expression and is associated with response to immunotherapy. *Nat Commun* **10**, 1125 (2019).
3. J.-Y. Xu *et al.*, Integrative Proteomic Characterization of Human Lung Adenocarcinoma. *Cell* **182**, 245–261.e217 (2020).

Table S1. Baseline demographic characteristics of the patients with benign lung diseases.

Related to Figure 1 and 3.

Characteristics	n (%)
Total	12 (100)
Sex	
Male	12 (100)
Female	0
Age, year	
Median (range)	54.5 (33 – 73)
Smoking	
Smoker, n (%)	6 (50)
Nonsmoker, n (%)	6 (50)
Histology, n (%)	
Pulmonary chronic inflammation (PCI)	8 (66.7)
Proliferation of alveolar epithelia and lymphoid tissue with carbon sedimentation	1 (8.3)
Fibrotic tubercle with carbon sedimentation	1 (8.3)
Inflammatory cell infiltration and cellulose exudation	1 (8.3)
Pulmonary carbon sedimentation and aggregation of phagocyte	1 (8.3)

Table S2. Baseline demographic characteristics of the patients whose samples were analyzed by immunohistochemistry assay. Related to Fig. 1c, d.

Characteristics	Patients, n (%)	MHC-I-low, n (%)	*P* values
Total	33	22 (66.7)	
Gender			
Male	11 (33.3)	7 (63.6)	0.39
Female	11 (33.3)	5 (45.5)	
Unknown	11 (33.3)	10 (90.9)	
Age			
<60	15 (45.5)	10 (66.7)	0.09
≥60	7 (21.2)	2 (28.6)	
Unknown	11 (33.3)	10 (90.9)	
Smoking			
Smoker	12 (36.4)	10 (83.3)	0.08
Non-smoker	17 (51.5)	9 (52.9)	
Unknown	4 (12.1)	3 (75.0)	
Histology			
LUAD	23 (69.7)	13 (56.5)	0.16
LUSC	7 (21.2)	6 (85.7)	
Carcinoid	1 (3.0)	1 (100)	
Unknown	2 (6.1)	2 (100)	
TNM stage			
I-II	15 (45.5)	10 (66.7)	0.81
III-IV	16 (48.5)	10 (62.5)	
Unknown	2 (6.0)	2 (100)	
Exposure			
Non-smoker	10 (30.3)	4 (40.0)	0.03*
Smoker	9 (27.3)	7 (77.8)	
Patients from HAP region	14 (42.4)	11 (78.6)	

LUAD, lung adenocarcinoma; LUSC, lung squamous cell carcinoma. *, *P* values were determined by chi-square test.

Table S3. Baseline demographic characteristics of the patients with lung cancer whose samples were detected by Western blot in Fig. 1e, f. The expression of MHC-I is normalized to GAPDH.

Characteristics	Patients, n (%)	MHC-I-low*, n (%)	*P* values
Total	28	21 (75.0)	
Gender			
Male	21 (75.0)	17 (81.0)	0.21
Female	7 (25.0)	4 (57.1)	
Age			
<60	15 (53.6)	10 (66.7)	0.27
≥60	13 (46.4)	11 (84.6)	
Smoking			
Smoker	20 (71.4)	17 (85.0)	0.05
Non-smoker	8 (28.6)	4 (50.0)	
Histology			
LUAD	15 (53.6)	12 (80.0)	0.51
LUSC	13 (46.4)	9 (69.2)	
TNM stage			
I-II	17 (60.7)	14 (82.4)	0.26
III-IV	11 (39.3)	7 (63.6)	

*, The median MHC-I expression level in nonsmokers served as the cutoff to dichotomize tumors into MHC-I-high and MHC-I-low groups.

Table S4. Baseline demographic characteristics of the patients whose samples were analyzed by Multiplex Immunohistochemistry assay for MHC-I, MARCH4, and CD8.

Related to Fig. 1g, h, 3o-q.

Characteristics	Patients, n (%)	MHC-I-low*, n (%)	*P* values
Total	51	30 (58.8)	
Gender			
Male	29 (56.9)	24 (82.8)	6.68-05
Female	22 (43.1)	6 (27.3)	
Age			
<60	22 (43.1)	11 (50.0)	0.26
≥60	29 (56.9)	19 (65.5)	
Smoking			
Smoker	23 (45.1)	18 (78.3)	0.01
Non-smoker	28 (54.9)	12 (42.9)	
Histology			
LUSC	50 (98.0)	29 (58.0)	0.40
LASC	1 (2.0)	1 (100.0)	
TNM stage			
I-II	50 (98.0)	30 (60.0)	0.23
III	1 (2.0)	0 (0.0)	

ASC, lung adenosquamous carcinoma. * The median MHC-I expression level in nonsmokers served as the cutoff to dichotomize tumors into MHC-I-high and MHC-I-low groups.

Table S5. Baseline demographic characteristics of the patients whose samples were analyzed by Multiplex Immunohistochemistry assay for MHC-I, CD8, and GZMB.

Related to Fig. S2a-e.

Characteristics	Patients, n (%)
Total	66
Gender	
Male	60 (90.9)
Female	6 (9.1)
Age	
<60	26 (39.4)
≥60	39 (59.1)
Unknown	1 (1.5)
Histology	
LUSC	66 (100)
TNM stage	
I-II	46 (69.7)
III	20 (30.3)

* The smoking status of the patients was not included in this table by the tissue microarray provider.

273 **Table S6. Reagents used in this study.** The 223 clinically available drugs were purchased

274 from Selleck Chemicals LLC (Houston, TX, USA) and were listed in Table S8.

Reagents	Source	Identifier
Carcinogens		
Butadiene	Energy Chemical	cat#W420325-100ML
Vinyl chloride	Aladdin	cat#V128313-1ML
Ethylene oxide	Aladdin	cat#E298673-1ML
Formaldehyde	Aladdin	cat#F111939-2ML
Benzo[a]pyrene	Sigma-Aldrich	cat#B1760-1G
N-Methyl-N′-nitro-N-nitrosoguanidine	MLC	cat#MG17400-5g
N'-Nitrosonornicotine	Macklin	cat# N916948
Dibenzo(a,h)anthracene	Sigma-Aldrich	cat# 91861
Nicotine	Absin	cat#440649
Benzo(ghi)perylene	Sigma-Aldrich	cat#B9009
1,2-Dimethylhydra-zine	JSENB	cat#ES-D161802
Polyhexamethyleneguanidine	MLC	cat#MG58914-100g
4-(methylnitrosamino)-1-(3-pyridyl)-1-butanone	Sigma-Aldrich	cat# 78013
Compounds		
Cycloheximide	Selleck	cat#S7418
MG132	Selleck	cat#S2619
Retinoic acid	Selleck	cat#S1653
Bexarotene	Selleck	cat#S2098
Chloroquine	Selleck	cat#S6999
Reagents used in cellular experiments		
RPMI 1640	Gibco	cat#31800-014
DMEM	Gibco	cat#12800-017
Fetal Bovine Serum	Gibco	cat#10099158
Dimethyl sulfoxide	Sigma-Aldrich	cat#472301-4L
BSA	Roche	cat#AP0027
0.25% Trypsin-EDTA	Gibco	cat#25200-72
Tween-20	Amresco Inc.	cat#0777
DAPI	Incitrogen	cat#2305156
Collagenase IV	Sigma-Aldrich	cat#C4-22-1g
TEMED	Solarbio	cat#T8090
NCM Universal Antibody Diluent	NCM Biotech	cat#WB500D
Ncm ECL Ultra	NCM Biotech	cat#P10300
Triton X-100	Solarbio	cat#T8200
Acryl/Bis 30% Solution (29:1)	Sangon Biotech	cat#B546017
Protein Ladder	ThermoFisher	cat#26616
SDS	JiSiEnBei	cat#JS0054-500G
Phosphatase inhibitors	Bimake	cat#B15001

Penicillin-Streptomycin 100× solution	Gibco	cat#15140-122
Trypsin	Gibco	cat#25200-72
16% Formaldehyde Solution (W/V), Methanol-free	ThermoFisher	cat#28908
Protease Inhibitor Cocktail	Roche	cat#04693159001
Ammonium persulfate	BioMOL	cat#H8N208S2
Yeast extract	OXOID.	cat#LP0021
Tryptone	OXOID	cat#LP0042
protein A/G agarose	Santa Cruz Biotechnology	cat#sc-2003
TRIzol Reagent	Invitrogen	cat#15596018
Phosphate-buffered saline	HyClone	cat#SH30256.12
Hematoxylin	ZSGB-Bio	cat#ZLI-9610
Lipofectamine™ 3000	ThermoFisher	cat#L3000001
EDTA antigen retrieval solution (50×)	WEIAOBIO	cat#WH1034
Polyethylenimine, branched	Sigma-Aldrich	cat#408727-100ML
Peroxidase Blocking Solution	ZSGB-Bio	cat#ZLI-9311
Kits and reagents		
DNA Gel Extraction Kit	Axygen	cat#AP-GX-50
eECL Western Blot Kit	CWBIO	cat#CW0049M
sCelLiVE® Tissue Dissociation Kit	Singleron	cat#1190062
AllPrep DNA/RNA Mini Kit	Qiagen	cat#80204
GeneJET Gel Extraction Kit	Thermo Fisher Scientific	cat#K0691
MultiS One-step Cloning Kit	Vazyme	cat#C113
HiScript III RT SuperMix for qPCR (+gDNA wiper)	Vazyme	cat#R323
2 × Rapid Taq Master Mix	Vazyme	cat#P222
HiFiScript cDNA Synthesis Kit	Vazyme	cat#R312
SYBR® Premix Ex Taq™	Vazyme	cat#Q712
Plasmid Midi Preparation Kit	CWBio	cat#CW21055
Multiplex fluorescent immunohistochemistry kit	Panovue	cat#10004100100

275

Table S7. Baseline demographic characteristics of the patients with lung cancer whose samples were detected by Western blot analyses. Related to Fig. 3l-n. The expression of MARCH4 is normalized to GAPDH.

Characteristics	Patients, n (%)	MARCH4-high, n (%)	*P* values
Total	47	29 (61.7%)	
Gender			
Male	35 (72.9)	23 (65.7)	0.33
Female	12 (27.1)	6 (50.0)	
Age			
<60	31 (66.7)	17 (54.8)	0.18
≥60	16 (33.3)	12 (75.0)	
Smoking			
Smoker	31 (64.6)	23 (74.2)	0.01
Non-smoker	16 (35.4)	6 (35.3)	
Histology			
LUAD	27 (58.3)	17 (63.0)	0.60
LUSC	17 (35.4)	12 (70.6)	
LASC	3 (6.3)	0 (0)	
TNM stage			
I-II	26 (60.4)	16 (51.5)	0.98
III-IV	21 (39.6)	13 (61.9)	

*, The median MMARCH4 expression level in nonsmokers served as the cutoff to dichotomize tumors into MARCH4-high and MARCH4-low groups.

Table S9. Primers, shRNAs, and siRNAs used in the study

Target	Forward primer (5'→3')	Reverse primer (5'→3')
Primers		
CDHR3	TTACCTGCTACAGGCAATGTG	CCTGACAGCCAATTCACCCTAA
SCGB1A1	TTCAGCGTGTCATCGAAACCC	ACAGTGAGCTTTGGGCTATTTTT
MUC5B	GCCCACATCTCCACCTATGAT	GCAGTTCTCGTTGTCCGTCA
ZG16B	TGCAGCCAGGCGAATACATC	GGTCGGCTCCTCTAGTGGATA
KRT5	TGACCTCCGCAACACCAAG	CAGATTGGCGCACTGTTTCTT
SCGB3A2	AAGCTGGTAACTATCTTCCTGCT	AGGGGCACTTTGTTGATGAGG
FOXJ1	GCCTCCCTACTCGTATGCCA	GCCGACAGGGTGATCTTGG
SPDEF	CAGTGCCCGGTCATTGACA	CAGCCGGTATTGGTGCTCT
NOTCH1	GAGGCGTGGCAGACTATGC	CTTGTACTCCGTCAGCGTGA
NOTCH2	CCTTCCACTGTGAGTGTCTGA	AGGTAGCATCATTCTGGCAGG
NOTCH3	TGGCGACCTCACTTACGACT	CACTGGCAGTTATAGGTGTTGAC
CDC20B	CAAGATTCCGCCAACGTACTC	CCTTGTGGTAATGGGGCTACT
NGF	GGCAGACCCGCAACATTACT	CACCACCGACCTCGAAGTC
MYB	GAAAGCGTCACTTGGGGAAAA	TGTTCGATTCGGGAGATAATTGG
MUC5AC	CAGCACAACCCCTGTTTCAAA	GCGCACAGAGGATGACAGT
MARCH1	CCAAGCTCAAACCCCTCCG	AGACCAAACCACACAGGTGAT
MARCH2	CACCGAGTGATGGTCCTTTCT	TCCAGACAGCTCTTATGCACG
MARCH3	AGAGCCCCTTCAATGACCG	GCAGCTCCGATGAATTGTCC
MARCH4	TTGGCTCATCTGGTCAACTTTC	GGTACACCGAGGGTCCTTCAT
MARCH5	GTCGGCTCTATCTATTGGACAGC	GCTCTCTCCATAACATCCAGACC
MARCH6	CACCTGAGAAACCGCTTTATCA	CCGTGAAGGCATATCTGGAGA
MARCH7	CTTCCCGAAGCAATACGCAG	TCGTTGTCCGCCTACCTTCA
MARCH8	AGTGACATTCCACGTCATTGC	GATCTCCTCAGCAGTACGGTC
MARCH10	GAGAAGAAACGCGATCAGTTTTG	TGGTTCAGTTAGAGCATCCTCC
MARCH11	CCGGGGAGAGTCTTCCACA	GCCTCATCCGATTGAACAGGT
MARCH9	ATCTCCCTGACGGTCATCGAG	GGCTGAAGGGCTGAGTGAG
TMG1	GCACCACACAGACGAGTATGA	GGTGATGCGATCAGAGGATTC
TGM2	CGTGACCAACTACAACTCGG	CATCCACGACTCCACCCAG
KRT10	ATGTCTGTTCGATACAGCTCAAG	CTCCACCAAGGGAGCCTTTG
KRT14	TGAGCCGCATTCTGAACGAG	GATGACTGCGATCCAGAGGA
P63	GGACCAGCAGATTCAGAACGG	AGGACACGTCGAAACTGTGC
mTMG1	GCTGTGCTCACGATCAGACC	AGGACTCATATTCCCGGTTCAA
mTMG2	CTAGAGGCTTCTACTGGCTACC	GCGTAAGGACATATTCCCGTC
mKRT10	CGAAGAGCTGGCCTACCTAAA	GGGCAGCGTTCATTTCCAC
mKRT14	AGCGGCAAGAGTGAGATTTCT	CCTCCAGGTTATTCTCCAGGG
mP63	CACCTGGACGTATTCCACCG	CATGGCACGGATAACAGCG
mAhR	GCCCTTCCCGCAAGATGTTAT	TCAGCAGGGGTGGACTTTAAT
WWP2	CAAAGCCCAAGGTGCATAATCG	CCAATGCGCTTCCCAGTCT
TCR8	TAGGCTTAATCACAGAGCTACCA	CTGCCAGGACAAACACTGTAT

TMEM129	CTCTGTCAACACTGAGTTCCG	GACTCCGTCACAGTCAGGTG
shRNAs		
sh*MARCH4-1*	CCAGTATTTCTTGGCTCATCT	AGATGAGCCAAGAAATACTGG
sh*MARCH4-2*	CGTCATCGCCATAAGCACAAA	TTTGTGCTTATGGCGATGACG
sh*RARβ2*-1	CCCAAGATGCTAATGAAGATT	AATCTTCATTAGCATCTTGGG
sh*RARβ2*-2	CAGCTTCCAGTTAGTGGATAT	ATATCCACTAACTGGAAGCTG
siRNAs		
si*RARa*-1	GCUUCCAGUUAGUGGAUAUTT	AUAUCCACUAACUGGAAGCTT
si*RARa*-2	GGGUGAUCACGCUGAAGAUTT	AUCUUCAGCGUGAUCACCCTT
si*RARβ2*-1	GGCCUUACCCUAAAUCGAATT	UUCGAUUUAGGGUAAGGCCTT
si*RARβ2*-2	GACCUUGAGGAACCGACAATT	UUGUCGGUUCCUCAAGGUCTT
si*MARCH4*-1	GGCUGGUACUGCUAUGGAUTT	AUCCAUAGCAGUACCAGCCTT
si*MARCH4*-2	GCCAGUAUUUCUUGGCUCATT	UGAGCCAAGAAAUACUGGCTT

283

Table S10. Antibodies used in this study.

Antibodies	Source	Identifier
Anti-MHC-I	Cell Signaling Technology	88274
Anti-MHC-I	abcam	70328
Anti-MARCH4	Santa Cruz Biotechnology	sc-514837
Anti-MARCH4	Thermo Fisher Scientific	PA5-23146
Anti-HLA-A	ABclonal	A11406
Anti-HLA-B	ABclonal	A1285
Anti-HLA-C	ABclonal	A1013
Anti-TGM1	proteintech	12912-3-AP
Anti-HLA-A	ABclonal	A2167
Anti-Cytokeratin14	abcam	Ab181595
Anti-Cytokeratin6A	proteintech	10590-1-AP
Anti-Cytokeratin10	abcam	76318
Anti-P63	abcam	ab124762
Anti-FOXJ1	proteintech	28443-1-AP
Anti-DNAI1	proteintech	12756-1-AP
Anti-SCGB1A1	proteintech	26909-1-AP
Anti-SCGB1A1	abcam	ab213203
Anti-MUC5AC	abcam	ab198294
Anti-AhR	proteintech	67785-1-Ig
Anti-GAPDH	proteintech	60004-1-Ig
Anti-Actin	proteintech	66009-1-Ig
Anti-HA	Cell Signaling Technology	3724
Anti-flag	Cell Signaling Technology	14793
Anti-Ub	Cell Signaling Technology	3936
Anti-SPDEF	proteintech	11467-1-AP
Anti-ZG16B	proteintech	20803-1-AP
FITC-CD3	biolegend	100203
PerCP-CD8	biolegend	100731
APC-CD45	biolegend	103116
PEcy7-CD4	biolegend	100527
BV421-CD62L	biolegend	104435
PE-CD44	biolegend	103007

Figures and legends

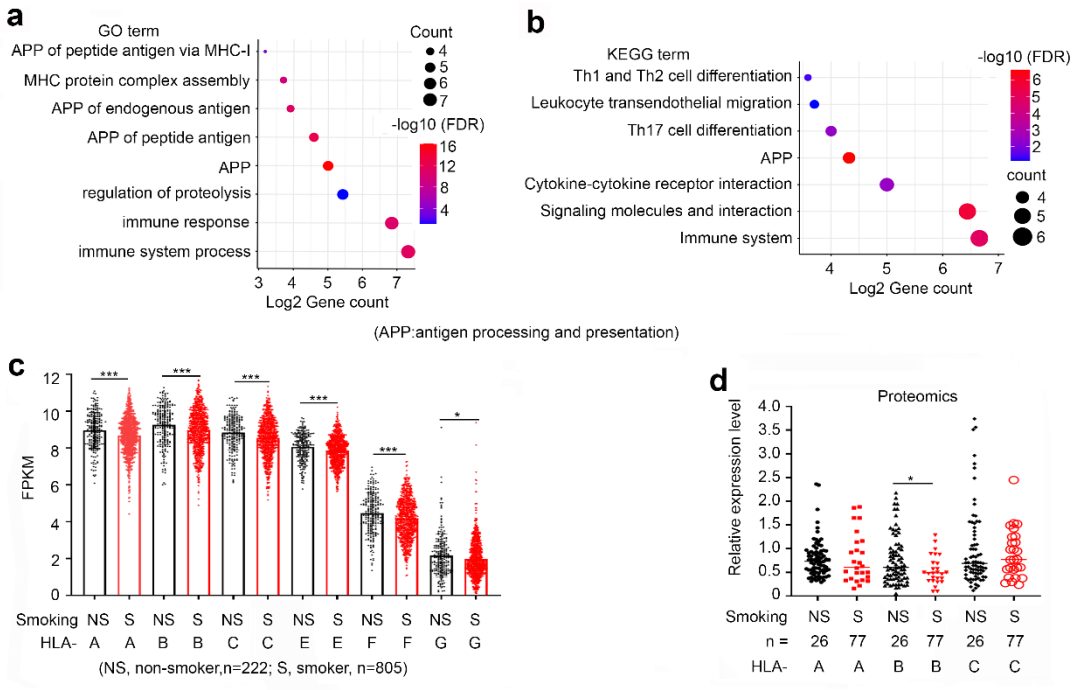

Fig. S1. Downregulation of MHC-I in individuals exposed to smohaze. (a-c) Analyses of differentially expressed genes in TCGA NSCLC datasets, comparing those in smokers with nonsmokers, revealed significant enrichments in Gene Ontology (GO) terms (a) and Kyoto Encyclopedia of Genes and Genomes (KEGG) pathways (b). The mRNA expression levels of *HLA-A*, *B*, *C*, *E*, *F*, and *G* were compared between tumor samples from smokers and nonsmokers (c). (d) The protein expression levels of HLA-A, B and C were compared between tumor samples from smokers and nonsmokers using NSCLC proteomic data (*3*). Error bar, SD. *, $P < 0.05$; ***, $P < 0.001$. Student's *t*-test.

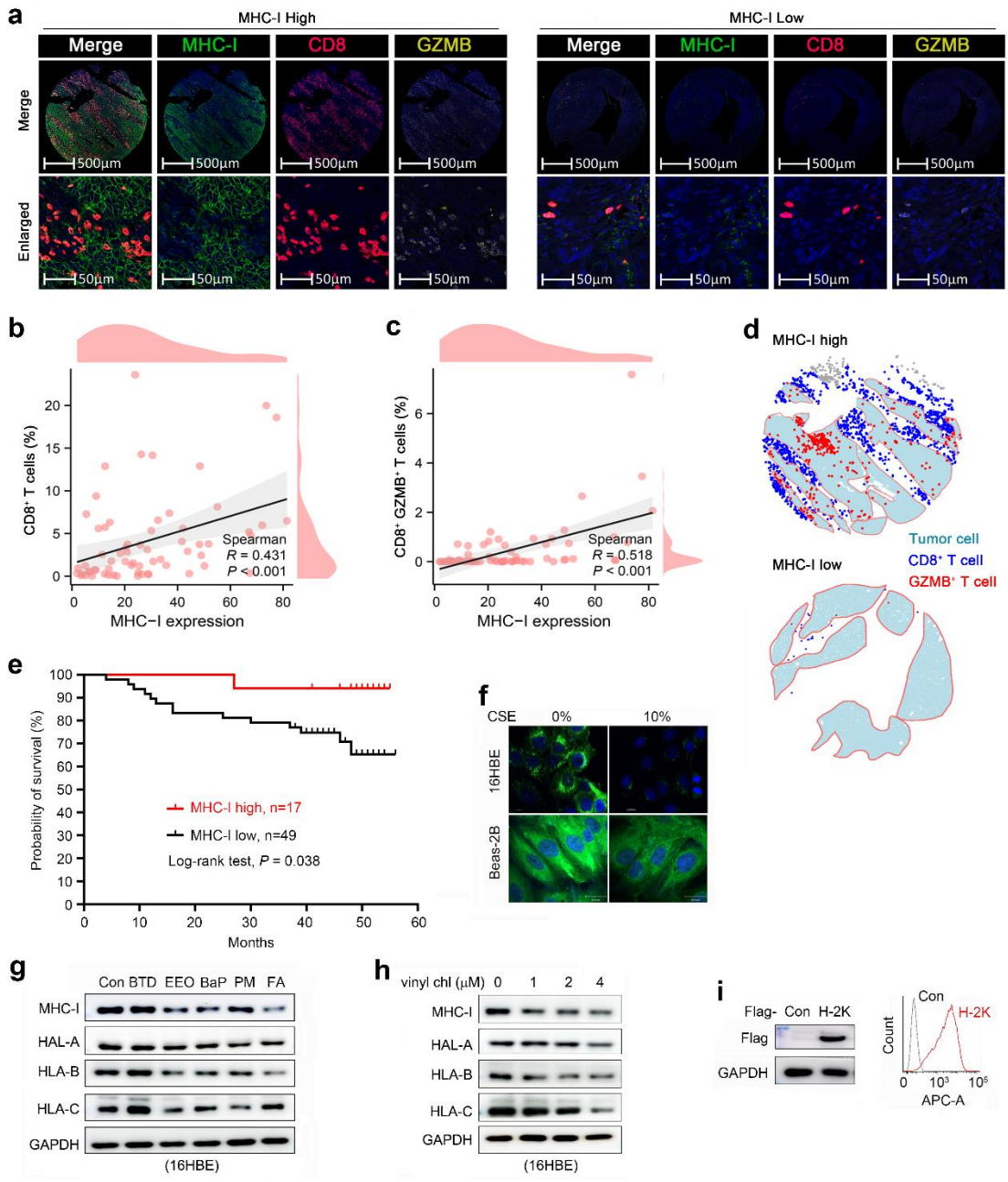

Fig. S2. MHC-I in LUSCs. (a) mIHC assays of a tissue microarray containing tumor samples harvested from 66 patients with untreated LUSC. (b, c) The correlation between the expression levels of MHC-I and $CD8^+$ (b) or $CD8^+GZMB^+$ (c) T cells in LUSCs. *P* values, Pearson's correlation test. (d) Tumor infiltration of $CD8^+$ and $CD8^+GZMB^+$ T cells in patients with high level- and low level- MHC-I. (e) The association between MHC-I expression level and the overall survival of the patients. (f) Immunofluorescence analyses of the effect of CSE on MHC-I expression in 16HBE and Beas-2B cells. (g) Effects of indicated carcinogens on

MHC-I components in 16HBE cells, detected by Western blot. BaP, benzo(a)pyrene; BTD, butadiene; EEO, ethylene oxide; FA, formaldehyde; PM, $PM_{2.5}$. (h) Effects of vinyl chloride on MHC-I components in 16HBE cells, detected by Western blot. (i) Overexpression of H-2K in M109 cells. Detected by WB (left) and flow cytometry (right) using carboxyfluorescein succinimidyl ester (CFSE)-propidium iodide (PI) staining. Related to Fig. 2i.

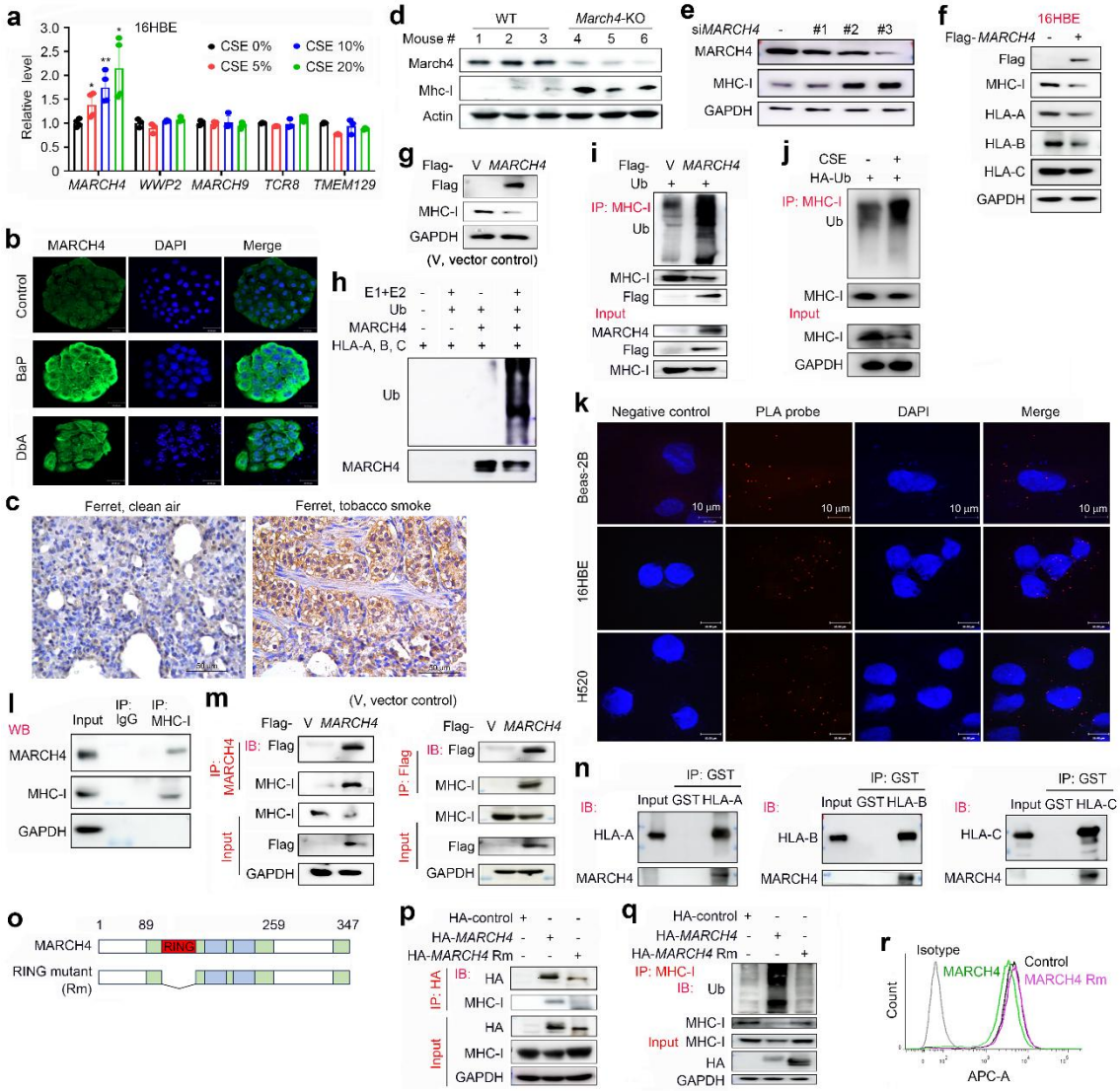

311

312 **Fig. S3. Air pollutants upregulate MARCH4 to suppress MHC-I. Related to Fig. 3.** (a)

313 16HBE cells were treated with CSE for 48 h, RNA samples were extracted, and subjected to

314 qRT-PCR to detect the expression of indicated genes. Error bar, SD. *, $P < 0.05$; **, $P < 0.01$.

315 Student's *t*-test. (b) Immunofluorescence analysis of the effects of BaP and DbA on

316 MARCH4 in 16HBE cells. (c) Representative IHC images displaying the expression of

317 MARCH4 in lung tissues of ferrets exposed to clean air or tobacco smoke. (d) WB analyses

318 of indicated proteins in wild-type and *March4*$^{-/-}$mice. (e) WB analyses of MHC-I expression

319 in Beas 2B cells that were transfected with si*MARCH4*. (f) WB analyses of MHC-I

components in 16HBE cells that were transfected with Flag-*MARCH4*. (g) WB analyses of MHC-I in 293T cells that were transfected with Flag-*MARCH4*. (h) An in vitro ubiquitination assay using E1, E2, ubiquitin, and HLA-A, B, C, in the absence or presence of MARCH4. (i) 293T cells were transfected with Flag-*MARCH4* and HA-Ub for 48 h, lysed, and subjected to co-IP and WB using indicated antibodies. (j) 293T cells were transfected with HA-Ub and treated with CSE for 48 h, lysed, and subjected to co-IP and WB using indicated antibodies. (k) Representative images of proximity ligation assay (PLA) using the Duolink in situ PLA Probe and anti-MHC-I/anti-MARCH4 antibodies in indicated cells. (l) Co-IP and WB assays using lysates of Beas 2B cells and indicated antibodies. (m) 293T cells were transfected with Flag-*MARCH4* for 48 h, lysed, and subjected to co-IP and WB. (n) Glutathione S-transferase (GST) pull-down and WB assays using GST-HLA-A, B, C, and Flag-MARCH4 proteins and indicated antibodies. (o) Schematic diagrams representing MARCH4 mutant constructs. (p-r) 16HBE cells were transfected with Flag-*MARCH4* or Flag-*MARCH4* Rm for 48 h, lysed, and subjected to co-IP and WB using indicated antibodies (p, q). (r) Flow cytometry of membranous MHC-I in cells transfected with Flag-*MARCH4* or Flag-*MARCH4* Rm.

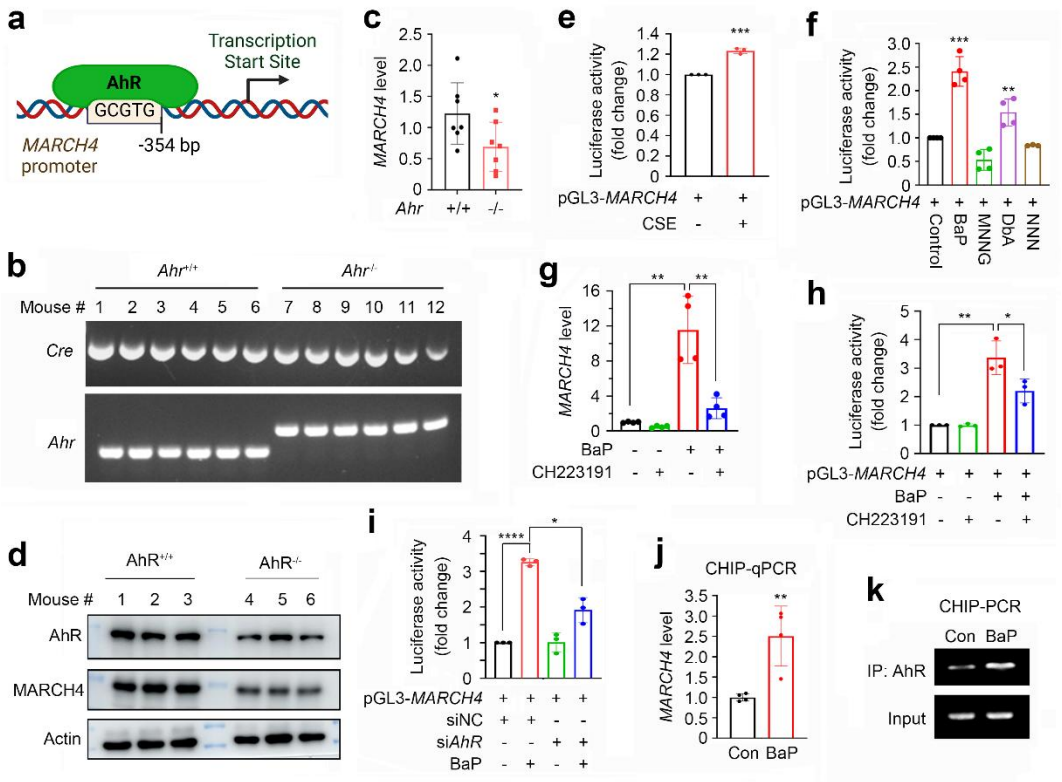

335

336 **Fig. S4. AhR mediates smohaze-induced upregulation of MARCH4.** (a) The potential

337 AhR-binding site in *MARCH4* promoter. (b) Confirmation of genotype in $Ahr^{+/+}$ and $Ahr^{-/-}$

338 mice. (c) qRT-PCR analyses of *March4* expression in lung tissues of $Ahr^{+/+}$ and $Ahr^{-/-}$ mice, in

339 which Ahr was knockout in alveolar type II cells. (d) WB analyses of March4 expression in

340 lung tissues of $Ahr^{+/+}$ and $Ahr^{-/-}$ mice. (e) Luciferase assay was performed in HLF cells

341 transfected with *MARCH4* promoter-luciferase reporter construct in the absence or presence

342 of CSE. (f) Luciferase assay was performed in HLF cells transfected with *MARCH4*

343 promoter-luciferase reporter construct in the absence or presence of indicated carcinogens. (g)

344 16HBE cells were treated with 5 μM BaP and/or 5 μM CH223191 for 48 h, lysed, and

345 subjected to qRT-PCR to test the expression of *MARCH4*. (h, i) Luciferase assay was

346 performed in HLF cells transfected with *MARCH4* promoter-luciferase reporter construct,

347 treated with BaP/CH223191 (h), or si*AhR*/BaP (i). (j, k) Chromatin immunoprecipitation

348 (ChIP) assays were performed in BaP-treated or untreated 16HBE cells. The enriched

MARCH4 was detected by qRT-PCR (j) and RT-PCR (k). Error bar, SD. *, $P < 0.05$; **, $P < 0.01$; ***, $P < 0.01$; ****, $P < 0.0001$. Student's *t*-test.

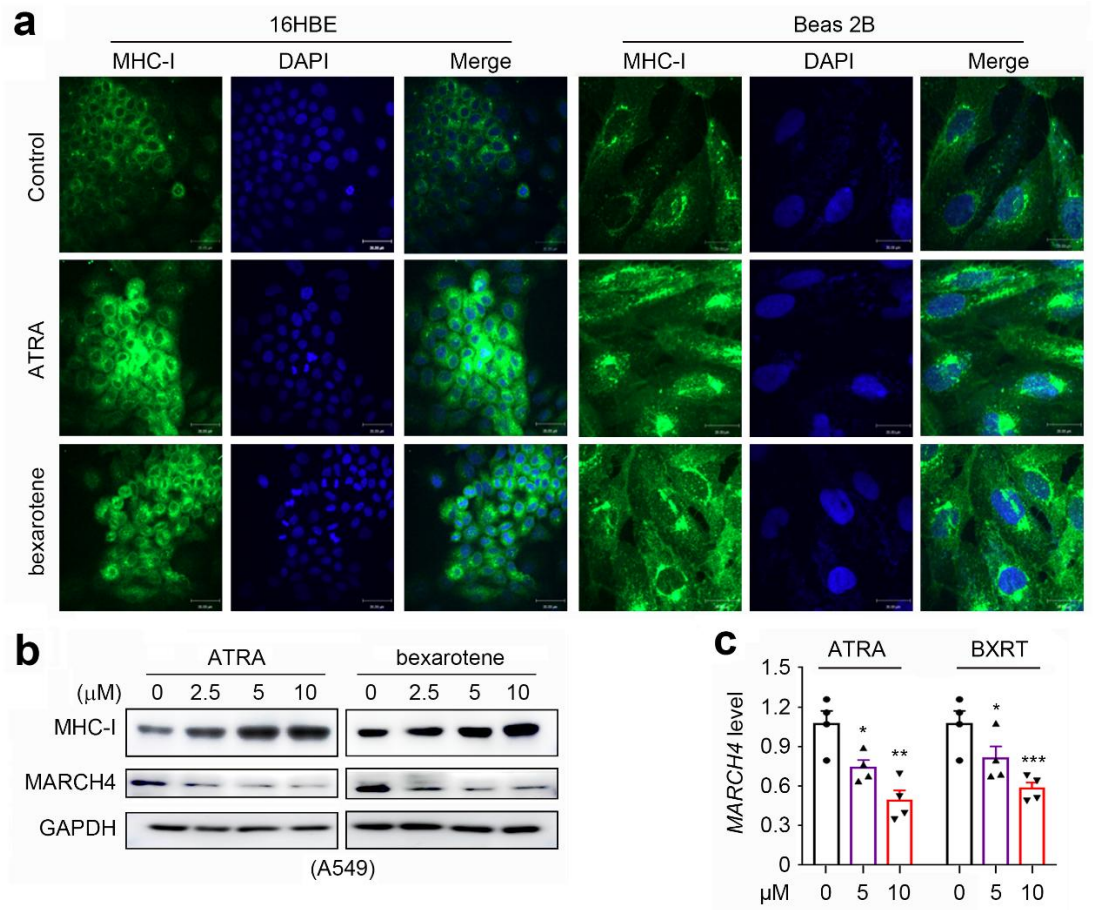

Fig. 5. Effects of ATRA/BXRT on MHC-I expression. (a) Immunofluorescence analyses of MHC-I in cells treated with 5 μM ATRA or BXRT for 48 h. DAPI was used to counterstain nucleus. (b) A549 cells were treated with ATRA or BXRT for 48 h, lysed, and subjected to WB using indicated antibodies. (c) Beas 2B cells were treated with ATRA or BXRT for 48 h, lysed, and subjected to qRT-PCR to test the expression of *MARCH4*. Error bar, SD. *, $P < 0.05$; **, $P < 0.01$; ***, $P < 0.001$. Student's *t*-test.

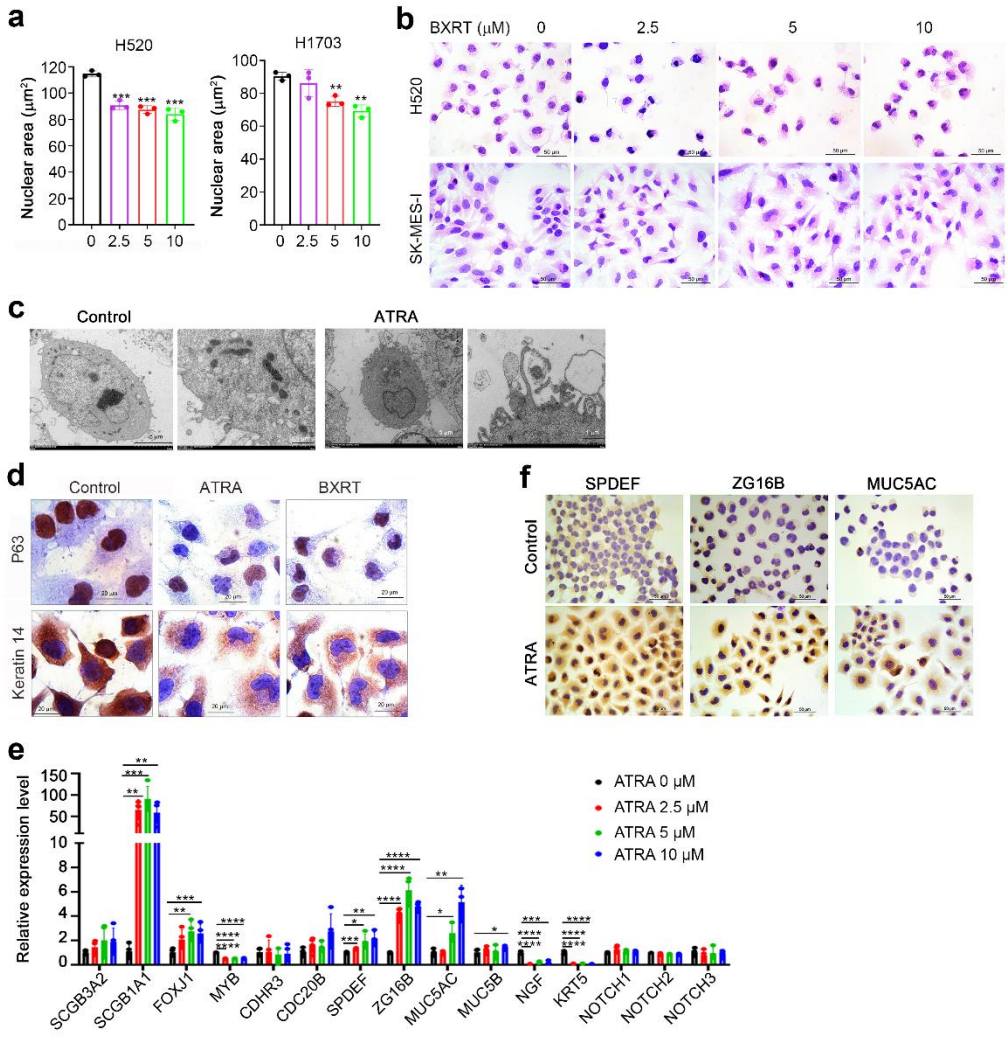

360

361 **Fig. S6. Effects of ATRA and BXRT on LUSC cells.** (a) The cells were treated with ATRA

362 at indicated concentration for 15 days, stained with H&E, and nucleus area was measured by

363 HALO software. (b) The cells were treated with BXRT for 15 days and those on coverslips

364 were stained with H&E, and imaged with a microscope. (c) H520 cells treated with 5 μM

365 ATRA for 15 days were harvested and processed for TEM to examine microvilli and cilia. (d)

366 The ATRA/BXRT-treated H520 cells were analyzed by IHC using indicated antibodies. (e)

367 H520 cells were treated with ATRA for 48 h, lysed, and subjected to qRT-PCR to test the

368 expression of indicated genes. Error bar, SD. *, $P < 0.05$; **, $P < 0.01$; ***, $P < 0.001$; ****,

369 $P < 0.0001$. Student's *t*-test. (f) H520 cells were treated with ATRA, and those grew on

coverslips were analyzed by IHC using indicated antibodies.

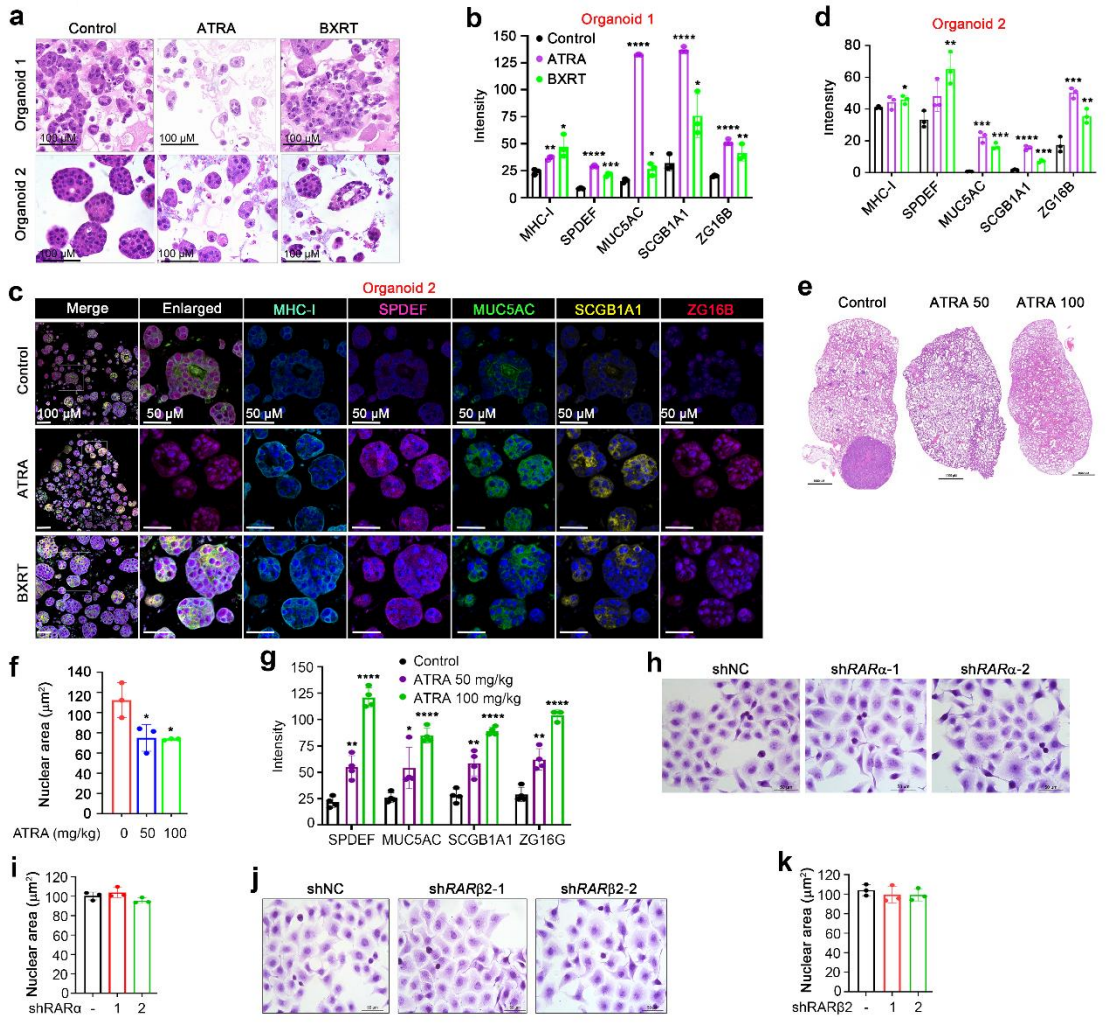

Fig. S7. ATRA and BXRT induce goblet-like differentiation of LUSC cells. (a) Effects of ATRA/BXRT on patient-derived organoids. Photographed by a microscope. (b) mIHC was performed in ATRA/BXRT-treated organoid 1, and changes in immunofluorescence intensity of indicated proteins are shown. (c, d) Organoid 2 derived from a 66-year-old female patient with poorly differentiated LUSC were treated with ATRA or BXRT for 15 days, fixed, and analyzed by mIHC for the expression of cell markers (c). Changes in immunofluorescence intensity of indicated proteins are shown (d). (e) H&E staining of lung tissues harvested from

H520-xenografted mice that were treated with ATRA. (f) Changes in nucleus area of tumor cells harvested from H520-xenografted NCG mice that were treated with ATRA. (g) Changes in protein immunofluorescence intensity of tumor cells harvested from H520-xenografted NCG mice that were treated with ATRA. (h-k) H520 cells were transfected with sh*RARα* (h, i) or sh*RARβ2* (j, k), stained with H&E, and evaluated with a microscope. Error bar, SD. *, $P < 0.05$; **, $P < 0.01$; ***, $P < 0.001$; ****, $P < 0.0001$. Student's *t*-test.

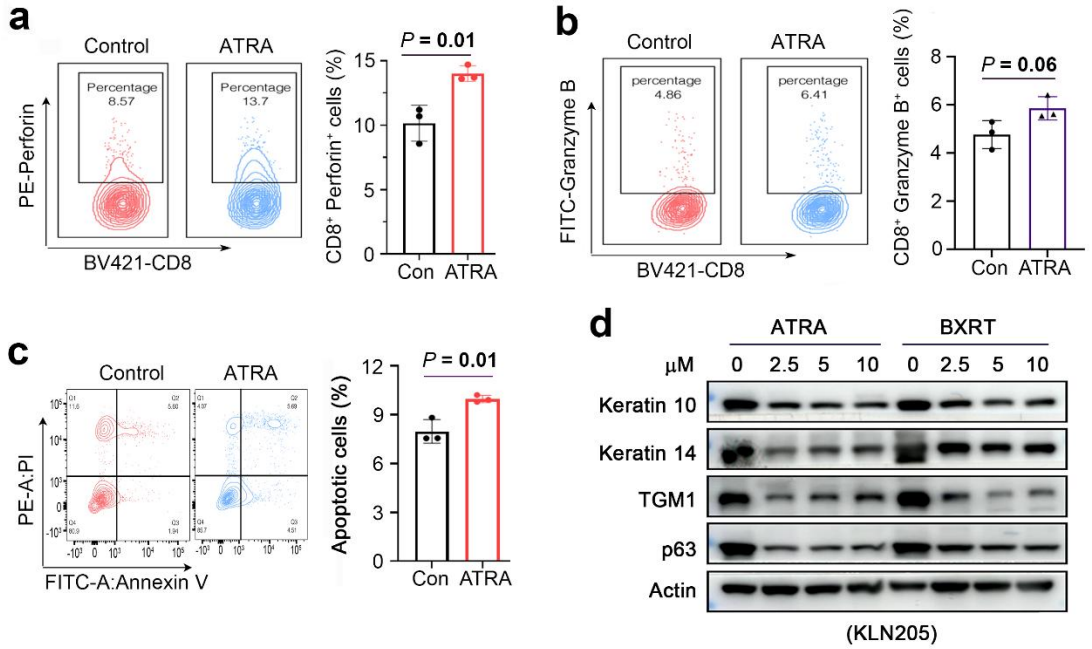

Fig. S8. Effects of ATRA on immune cells. (a-c) Co-culture of ATRA-treated H520 cells with $CD8^+$ T cells and dendritic cells (DCs) that were derived from a healthy donor. The proportion of $CD8^+$ $Perforin^+$ T (a), $CD8^+GZMB^+$ T (b), and apoptotic H520 cells (c) were analyzed by flow cytometry. Error bar, SD. *P* values, Student's *t*-test. (d) KLN205 cells were treated with ATRA/BXRT for 48h, lysed, and subjected to WB using indicated antibodies.

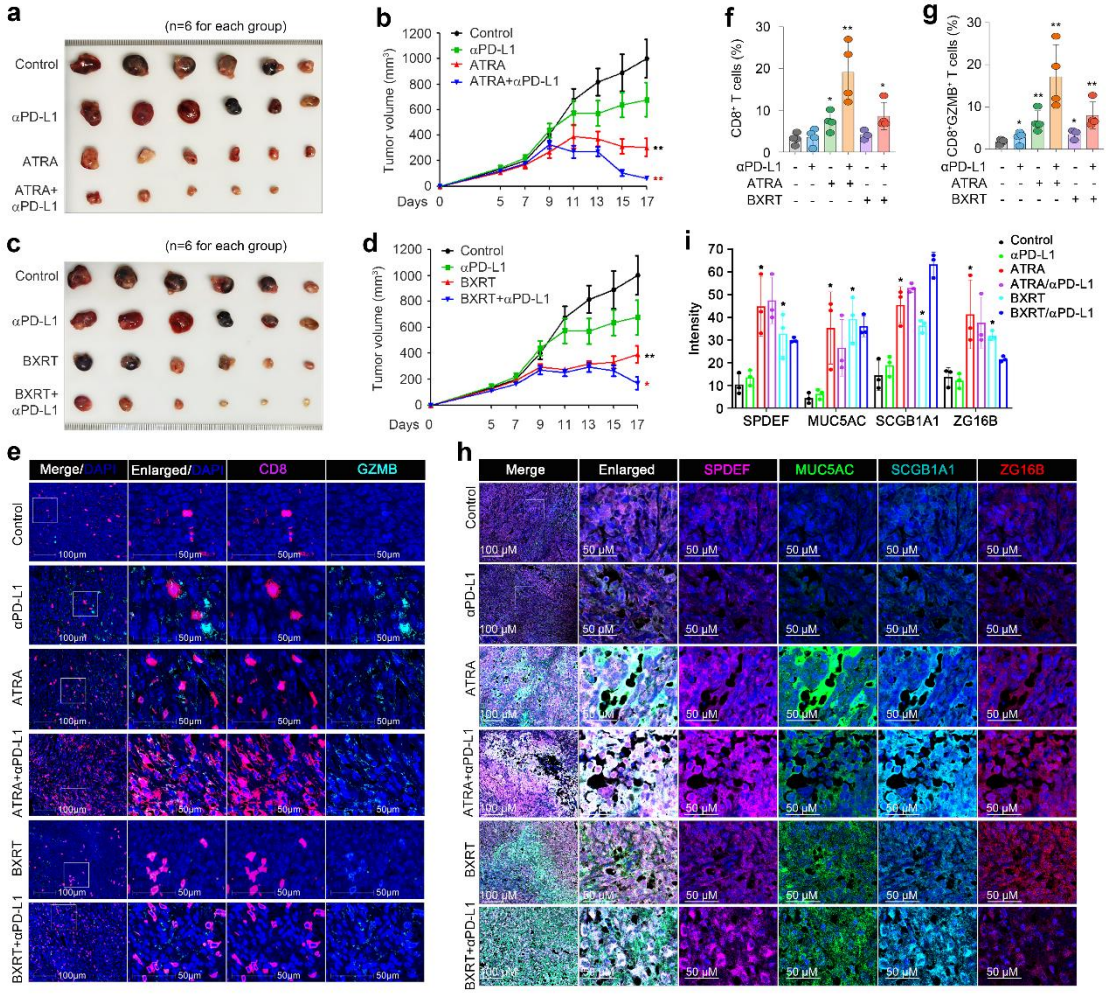

Fig. S9. Combined effects of retinoids and PD-L1 blockade in LUSC. (a-d) BALB/c mice were subcutaneously inoculated with 5×10^6 KLN205 LUSC cells and subsequently treated with ATRA/BXRT and anti-PD-L1 or anti-IgG antibody. Seventeen days later, the mice were sacrificed, tumors were resected and imaged (a, c). (b, d) Tumor volume was measured every two days. Data are shown as mean ± SD. *, P<0.05; **, P < 0.01. Two-way ANOVA. (e-g) mIHC analyses of CD8, GZMB, and DAPI in tumor tissues of the mice. Representative images are shown in (e), and the percentages of $CD8^+$ T or $CD8^+GZMB^+$ T cells in tumor tissues are displayed in (f, g). (h, i) mIHC analyses of SPDEF, MUC5AC, SCGB1A1, and ZG16B in tumor tissues of the mice. Representative images are shown in (h), and the intensity of the molecules are displayed in (i). Data are shown as mean ± SD. *, P<0.05; **, P <0.01.

405 Student's *t*-test.

406

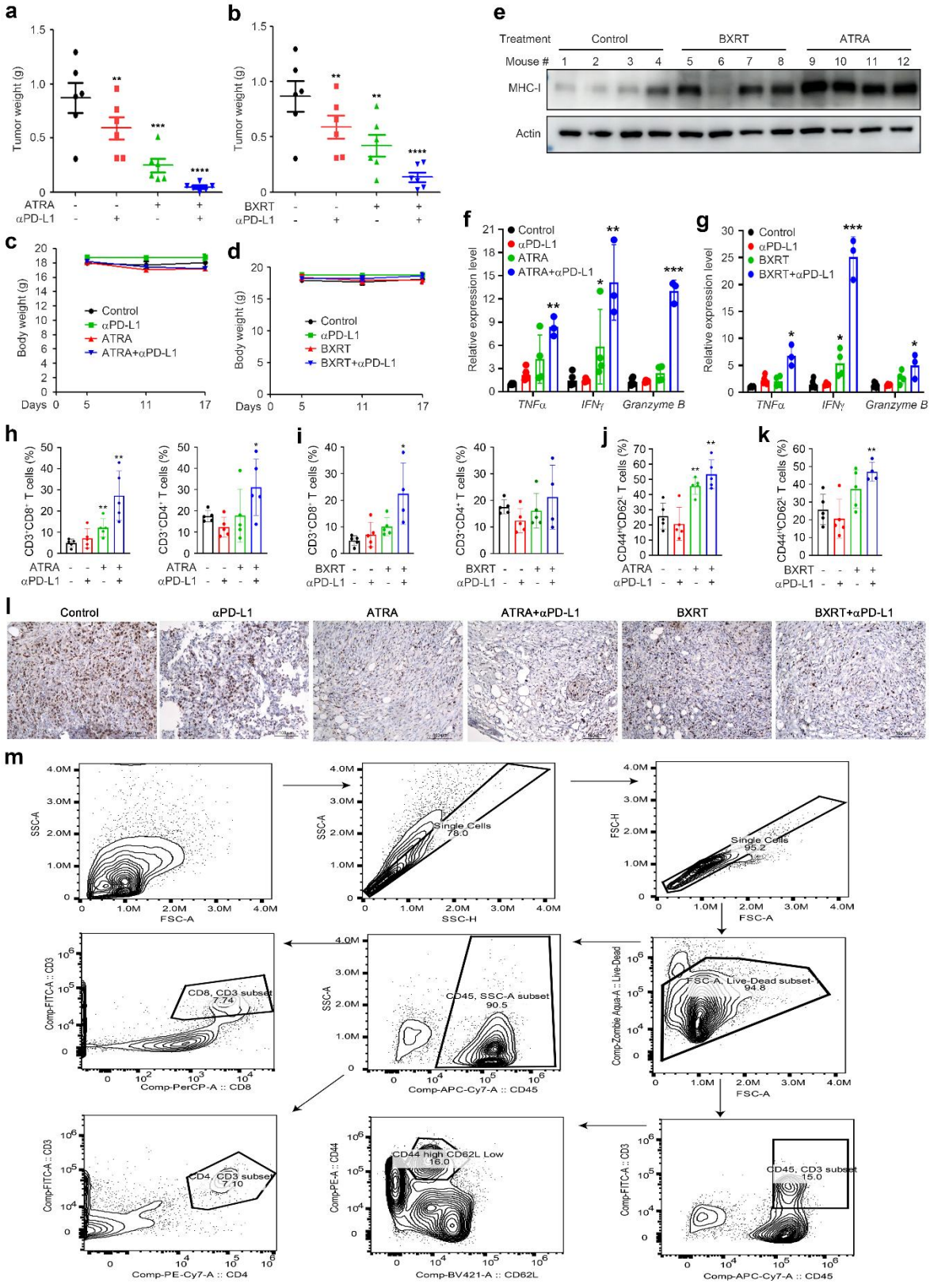

407

Fig. S10. Effects of retinoids on immune cells. (a, b) Tumor weight of KLN205 cell-bearing mice treated with ATRA/αPD-L1 (a) or BXRT/αPD-L1 (b). (c, d) Body weight of H520 cell-bearing mice treated with ATRA/αPD-L1 (c) or BXRT/αPD-L1 (d). (e) MHC-I expression in $CD45^-$ tumor cells isolated from KLN205 cell-bearing mice upon ATRA/BXRT were analyzed by WB. (f, g) Tumor tissues of KLN205 cell-bearing mice treated with ATRA/αPD-L1 (f) or BXRT/αPD-L1 (g) were lysed and subjected to qRT-PCR to test the expression of indicated genes. (h, i) Flow cytometry of $CD3^+CD8^+$ and $CD3^+CD4^+$ T cells in the tumor tissues harvested from KLN205 cell-bearing mice treated with ATRA/αPD-L1 (h) or BXRT/αPD-L1 (i). (j, k) Flow cytometry of $CD44^{high}CD62^{Low}$ T cells in tumor tissues harvested from mice treated with ATRA/αPD-L1 (j) or BXRT/αPD-L1 (k). (l) Ki-67 expression was analyzed by IHC in tumor tissues harvested from the mice. (m) Representative gating strategy for determination of different immune cell populations.

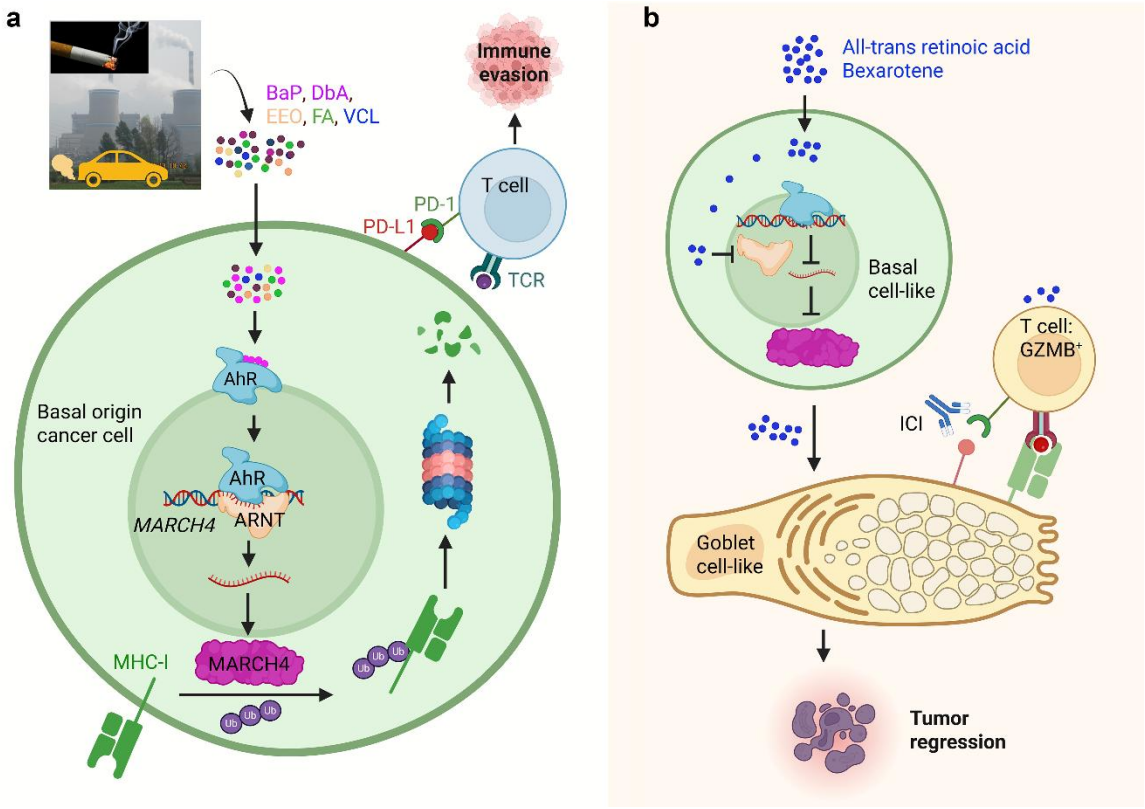

421

422 **Fig. S11. Schematic representation of smohaze-induced MHC-I downregulation and**
423 **retinoid-triggered goblet-like differentiation of LUSC cells.** (a) AhR mediates air
424 pollutant-induced upregulation of MARCH4, which causes ubiquitination and proteasomal
425 degradation of MHC-I. Air pollutants also induce upregulation of PD-L1 to induce immune
426 evasion of cancer cells (*2*). (b) Retinoids upregulate MHC-I and induce a MARCH4-
427 dependent differentiation of LUSC cells into goblet-like cells, synergizes with ICI, and cause
428 regression of tumors in vivo.